Mutation of *PFN1* gene in an early onset, polyostotic Paget's-like disease

Merlotti Daniela[1*], Materozzi Maria[1,2*], Bianciardi Simone[1], Guarnieri Vito[3], Rendina Domenico[4], Volterrani Luca[1], Bellan Cristiana[5], Mingiano Cristian[1], Picchioni Tommaso[1], Frosali Alessandro[1], Orfanelli Ugo[2], Cenci Simone[2], Gennari Luigi[1].

[1]*Department of Medicine Surgery and Neurosciences, University of Siena, Italy;* [2]*Division of Genetics and Cell Biology, San Raffaele Scientific Institute, Milan, Italy;* [3]*Medical Genetics Service, IRCCS "Casa Sollievo della Sofferenza" Hospital, San Giovanni Rotondo (FG), Italy;* [4]*Department of Clinical and Experimental Medicine, Federico II University Medical School, Naples, Italy;* [5]*Department of Medical Biotechnologies, University of Siena, Italy.*

*These authors contributed equally to this work

Email addresses: dmerlotti@yahoo.it; maria.materozzi@hotmail.it; s.bianciardi@gmail.com; v.guarnieri@operapadrepio.it; domenico.rendina@unina.it; luca.volterrani@unisi.it; cristiana.bellan@unisi.it; christian.mingiano@gmail.com; picchioni2@gmail.com; frosali5@gmail.com; orfanelli.ugo@hsr.it; cenci.simone@hsr.it; luigi.gennari@unisi.it.

Correspondence and Reprint Requests:

Daniela Merlotti, MD, PhD

Department of Medicine, Surgery and Neurosciences, University of Siena, Siena, Italy

Policlinico Santa Maria alle Scotte, Viale Bracci 53100 Siena ITALY

Tel. +390577585364; Fax. +390577233447

Email: dmerlotti@yahoo.it

FUNDINGS

This work was supported by the ASBMR Rising Star Award (to DM) and partly by Regione Toscana-ITT 2013 Grant (to LG) and the Italian Association of Patients with Paget's Disease of Bone (AIP) (to DM)

DISCLOSURE SUMMARY

MM, SB, VG, DR, LV, CB, CM, TP, AF, UO, and SC have nothing to declare. DM received honoraria from UCB Pharma and Savio Pharma. LG received honoraria from Sandoz

ABSTRACT

Context: Paget's disease of bone (PDB) is a metabolic bone disease, whose genetic cause remains unknown in up to 50% of familial cases.

Objective: Our aim was to investigate the underlying genetic defect in a large pedigree with a severe, early onset, autosomal dominant form of PDB across three generations.

Methods: Whole exome sequencing was performed in affected and unaffected family members, and then mutation screening was replicated in a sample of PDB cases with early-onset, polyostotic PDB.

Results: We identified a frameshift D107Rfs*3 mutation in *PFN1* (encoding for profilin1, a highly conserved regulator of actin-polymerization and cell motility) causing the truncation of the C-terminal part of the protein. The mutation was also detected in a 17-yrs old asymptomatic family member that upon biochemical and radiological analyses was indeed found to be affected. Sequencing of the entire *PFN1* coding region in unrelated PDB cases identified the same mutation in one patient. All mutation carriers had a reduced response to bisphosphonates, requiring multiple zoledronate infusions to control bone pain and achieve biochemical remission over a long term. In vitro osteoclastogenesis in PBMCs from mutation carriers showed a higher number of osteoclasts with PDB-like features. A similar phenotype was observed upon *PFN1* silencing in murine bone marrow-derived monocytes, suggesting that the frameshift *PFN1* mutation confers a loss of function in profilin 1 activity that induces PDB-like features in the osteoclasts, likely due to enhanced cell motility and actin ring formation.

Conclusions: Our findings indicate that *PFN1* mutation causes an early onset, polyostotic PDB-like disorder.

Keywords: Paget's disease of bone, *PFN1* gene, whole exome sequencing, bisphosphonates, osteoclast

INTRODUCTION

Paget's disease of bone (PDB, OMIM 602080), is a focal metabolic bone disease characterized by excessive and aberrant bone remodelling that ultimately leads to enlarged and deformed bones in one (monostotic form) or more (polyostotic form) regions of the skeleton [1]. As a result, bone pain, bone deformities (i.e., enlargement of the skull or bowing of the tibia), arthritis at adjacent joints, and fractures often occur. Moreover neoplastic degeneration of affected skeletal sites in osteosarcoma, or, less frequently, giant cell tumor has been described in 0.5%-1% of cases, an increase in the risk that, however, is several thousand-fold higher than in the general population [2, 3]. PDB affects both genders (with a slight predominance in males) and usually manifests after middle age, with a prevalence of around 1% or less in most Countries, although it remarkably increases with aging affecting up to 5% of the elder population in some areas [4]. This disorder was first described in 1876 by Sir James Paget [5] and remained an almost untreatable condition for about a century since the introduction of compounds with antiresorptive activity on bone, such as calcitonin and then bisphosphonates. In particular, the more recent development of potent intravenous nitrogen-containing bisphosphonates has remarkably improved treatment outcomes, relieving bone pain and allowing a long-term biochemical remission in the majority of patients [6, 7].

It is generally believed that the primary cellular abnormality in PDB resides in the osteoclasts, which contain up to 100 nuclei per cell and appear larger and more active than normal [8]. Moreover, pagetic osteoclasts precursors are hyper-responsive to different osteoclastogenic factors such as 1,25-dihydroxy-vitamin D, tumor necrosis factor (TNF)-α, or RANKL [9]. Despite the remarkable progresses occurred over the past two decades, the pathogenetic mechanisms of PDB remain in great part unknown and probably include the involvement of genetic and environmental

factors [1, 10, 11]. To date, mutations in *SQSTM1* and, less frequently, other genes have been associated to PDB, particularly in cases with a documented family history for the disorder [1]. However, the genetic causes are still unknown in up to 50% of familial PDB cases, suggesting the presence of additional predisposition genes. During the past years we identified different PDB pedigrees which resulted negative for the presence of *SQSTM1* mutations as well as for the newly identified *ZNF687* mutation [12] or mutations in other genes associated with rare inherited bone disorders showing phenotypic overlap with classical PDB (e.g. familial expansile osteolysis, expansile skeletal hyperphosphatasia, juvenile Paget's disease and multisystem proteinopathy) [13].

We now report the identification of a heterozygous frameshift mutation in a new gene, *PFN1*, associated with a severe, early onset, form of PDB in a large pedigree with a high penetrance, autosomal dominant pattern of inheritance.

PATIENTS AND METHODS

Study Population

This study included a pedigree with eight early-onset, polyostotic PDB cases, showing an autosomal dominant pattern of inheritance across three generations (Figure 1). The clinical and laboratory data were summarized in Table1. Five patients (II.2, II.4, II.6, III.1, III.2) and five healthy members (I.1, II.1, II.3, III.2, III.7) from three generations were recruited for Next Generation Exome Sequencing analysis. Members IV.3 and IV.4 in the fourth generation were sequenced but excluded from the segregation analysis due to their young age (below 20 yrs).

Then, we extended the mutation screening to all familial PDB cases selected from the large cohort of the Italian PDB Registry (including 893 unrelated PDB patients) with a reported diagnosis below age 50, for which mutation in all known genes affected in PDB or PDB-like diseases had been excluded. Overall, 41 patients meeting the above characteristics were selected, to which 3 patients with neoplastic degeneration in osteosarcoma were added, because of the reported history of sarcomatous degeneration of PDB in an affected pedigree member (Pt. I.2).

The study was approved by the ethics institutional review board at the Policlinico Le Scotte Hospital of Siena and written informed consent was obtained from patients and their family members. If patients or family members were under 18 years old, the consent was obtained from their parents.

Genetic Analysis

Next Generation Exome Sequencing: DNA was collected from patients from buccal swab or peripheral blood and extracted using the Quick-DNA Universal Kit (Zymo Research, D4069). The Whole Exome Sequencing (WES) was performed by the Center for Translational Genomics and Bioinformatics (CTGB, San Raffaele Scientific Institute in Milan). To perform WES analysis, libraries were captured using Agilent SureSelect-Human-All-Exon V.6 probes and run on HiSeq 2500 and NextSeq 500 platforms (Illumina). The raw sequencing reads were mapped to the human genome reference assembly b37 (hs37d5) using the Burrows-Wheeler aligner (BWA). Duplicate reads were marked and excluded from further analysis using Picard Tools (https://broadinstitute.github.io/picard/). Capture metrics were calculated using the program CalculateHsMetrics in Picard with Agilent design SureSelect Human All Exon V6 r2 (https://earray.chem.agilent.com/suredesign/). Variant calling was performed using the tool Freebayes version 1.0.2 (Garrison E, Marth G. Haplotypebased variant detection from short-read sequencing. arXiv preprint arXiv:1207.3907 [q-bio.GN] 2012), with the following parameters: F 0.2; C 2; q 20; genotype-qualities; min-repeat-entropy 1; report-genotype-likelihood-max. Only variants with high or moderate predicted impact or splice junction related predicted effect were considered. We performed segregation analysis and filtering for rare and likely protein-affecting variants (considering only variants < 0.005 reported frequency in GnomAD).

Allele Cloning and Sanger Validation: DNA from affected and unaffected members were amplified for *PFN1* exon2 by PCR with the following primers: 5'-TTTTCTGCACTAACGTCCC-3' and 5'-AAGACCCCAACAATCTACCT-3'. The PCR product was then cloned in pGEM®-T Vectors using its dedicated kit (Promega A3600) and transformed into competent cells. An average of 10 colonies per sample were extracted with NucleoSpin Plasmid QuickPure Kit Miniprep (Machery-Nagel, 740609.250) and sequenced in service by Eurofins Genomics, with the described primers.

In silico analysis: The functional context of the identified mutation was predicted using the default settings of Provean [14] and Mutation Taster [15] prediction algorithms. Secondary and tertiary structure of mutant profilin1 was predicted using SWISS MODEL (https://swissmodel.expasy.org) and compared to wild-type profilin1 (P07737).

PFN1 Mutation Screening: screening of the *PFN1* gene was performed by direct PCR amplification and sequencing of the three exons and exon-intron boundaries. Briefly, 200 ng DNA was PCR amplified separately with the following primers: F1: 5'-ttcttctggctcactccctg-3' and R1: 5'-ttgaatccaacgtgctgagc-3'; F2: 5'-gtctgactccccttcatgttg-3' and R2: 5'-tgggaatcttggtgcactga-3'; F3: 5-tctgttcctctccagcgttt-3' and R3: 5'-ccaccaatttgaccagcaca-3' in a total volume of 25 uL containing: 1X Buffer, 6,25 pmol dNTPs, 20 pmol primers (each) and 1 U Ampli-Taq Gold Polymerase (ThermoFisher). For all the exons the Tm was 56°C. Amplicons were purified with ExoSAP-IT (ThermoFisher) and directly sequenced with both the forward and reverse primers (Big Dye Terminator Cycle Sequencing Kit, v.1.0, ThermoFisher). Reactions sequences were run on an ABI Prism 3100 (ThermoFisher) and electropherograms through the Sequencer 4.10 software (Gene Codes Corporation) using as reference control the human coding sequence of the PFN1 gene (NM_005022, GRCh37).

In vitro Osteoclastogenesis

The bone marrow of C57BL6 WT mice was flushed from the femurs and tibias by centrifugation at full speed for 1 minute at 4°C. It was resuspended with complete alphaMEM (Gibco-Life Technologies) supplemented with 10% (heat inactivated) fetal bovine serum (Hyclone, SH30070.03), penicillin/streptomycin (100 µg/ml; Lonza, 17–602E), L-glutamine (2 mM; Gibco-Life Technologies, 25030–081), filtered through a cell strainer and centrifuged. Cells were then resuspended in medium and plated with 100ng/mL of mouse MCSF (Peprotech 315-02). After 48 hours the supernatant was removed and bone marrow-derived monocytes (BMMs) were expanded for 4 days. Osteoclastogenesis was induced culturing BMMs with medium containing 10ng/mL of MCSF and 100ng/mL of RANKL (Biolegend, 577102), replaced every two days. For resorption assay, cells were plated on dentin discs (ids AE-8050), and cultured as mentioned above for 15-21 days. Resorption pits were stained by 1% blue toluidine (Sigma-Aldrich T3260) aqueous solution.

Peripheral Blood Mononucleated Cells (PBMCs) from selected PDB cases and age- and sex-matched healthy controls were isolated using Ficoll-Paque PLUS (GE Healthcare, GE17-1440-03) by centrifugation 400g – 30 minutes – room temperature. Cells were then plated in DMEM (Sigma-Aldrich, D5671), 10% (heat inactivated) Fetal Bovine Serum (Euroclone, ECS0180L), 1% penicillin/streptomycin (Sigma-Aldrich, P0781), 1% L-glutamine (Sigma-Aldrich, G7513) with addition of 30ng/mL recombinant human M-CSF (PeproTech, 300-25) for 24 hours. After incubation, osteoclastogenesis was induced supplementing cells with 30ng/mL of recombinant human sRANKL (Peprotech, 310-01C). The PBMCs were cultured for 15 days, replacing medium every 3 days.

TRAP staining was performed after 7-8 days (murine) or 14-15 days (human) of differentiation, after which they were fixed 10 minutes in 4% paraformaldehyde, washed in dH2O and incubated with TRAP solution (387A Acid Phosphatase, Leukocyte TRAP Kit, SIGMA) for 15-30 minutes at 37°C and consequently washed. Osteoclasts were counted as TRAP+ multinucleated (≥3 nuclei) cells per well.

PFN1 Silencing and viral packaging

Lentiviral vectors were generated starting from Mission shRNAs (Sigma-Aldrich) expressing anti-PFN1 (TRCN0000011968) and mock shRNA (SHC002). HEK293T cells cultured in IMDM, supplemented with fetal bovine serum, penicillin/streptomycin and glutamine as described above, were transfected by CaCl2 HBS precipitation with plasmids ENV (VSV-G), pMDLg/pRRE, pCMV-Rev with either a mock or anti-PFN1 shRNA. Plasmid-calcium complexes were incubated on cells for 16hours after which the medium was replaced. After 24hrs, the medium was filtered (0.22µ) and the virus was collected by ultracentrifuge for 2h at 20.000 rpm at RT. Supernatant was discarded and dried pellet was resuspended in sterile PBS. Aliquots were stored at -80°C. Isolated BMMs were incubated with virus for 16 hours, after which the medium was replaced. After 3 days, cells were detached and plated for *in vitro* osteoclastogenesis, immunofluorescence and resorption assay as previously described.

Silencing was verified by western blot. Briefly, total protein lysates were collected lysing cells in Tris-Buffered Saline (TBS) 1% SDS with proteases inhibitors cocktail (Roche, 11836153001) for 5 minutes and homogenised by syringe-based method. Samples were quantified by BCA method and 10-30µg of proteins were loaded on 20% acrylamide gels and separated through SDS-PAGE. Proteins were then transferred on a nitrocellulose membrane (IB23001, Life Technologies) through electroblotting (2hours at 300mA) at 4°C. Membranes were blocked in a 5% milk 0.01% Tween in TBS (TBS-T) solution, and incubated overnight at 4°C with primary antibodies diluted in a 3% BSA (Bovine Serum Albumin) TBS-T solution. The following primary antibodies were used: mouse β-Actin (A1978, Sigma-Aldrich) and rabbit anti-profilin1 (Abcam, 133529). Membranes were washed with TBS-T and incubated for 1 hour at RT with secondary antibodies: anti-Rabbit AlexaFluor647, diluted 1:4000 in blocking solution. Signal was detected by FLA9000 (FujiFilm, Tokyo Japan).

Immunofluorescence

Osteoclastogenesis was induced on glass slides in 48wells plates with 50.000cells/well. Osteoclasts were washed in PBS and fixed in formalin for 10 minutes, permeabilized in 0.2% TritonX100 in PBS for 5 minutes and blocked in 10% goat serum, 4% bovine serum albumin in PBS for 1h at RT. Slides were then briefly washed and incubated with primary rabbit anti-Paxilin (abcam, ab2264) dil. 1:200 for 40 minutes at 37°C. Slides were then washed and incubated with secondary anti-rabbit AF488 dil. 1:1000 for 40 minutes at 37°C. Actin filaments were stained with Pahlloidin AF594 (Invitrogen, A12381) and nuclei were stained with DAPI (Invitrogen, D1306) in PBS for 15 minutes at RT.

Quantitative Real Time PCR

For RT-PCR, RNA was extracted from with Trizol (Invitrogen, 10296028) and 1000ng retrotranscribed with ImProm-II Reverse Transcriptase (Promega, A3800). qPCR were performed in 10 µL mix with 5 µl SYBR green I master mix (Roche, 04707516001) on Roche LightCycler 480 and 1 µl 5 µM primers. Data were analyzed on Roche LC480 software with Advance Relative Quantification. Mouse ACTB gene expression was used as normalizer in the analyses. Primers used were:PFN1 5'-CATCGTAGGCTACAAGGACTCG-3', 5'-CCAAGTGTCAGCCCATTGACGA-3' and ACTIN: 5'-CCGCGAGCACAGCTTCTTTG-3', 5'-AGTCCTTCTGACCCATTCCCAC-3'. Reactions were carried out in 20µL with MasterMix SYBR Green (Roche) and analysis of gene expression was performed with Roche LC480 software.

RESULTS

Identification of a *PFN1* pathogenic variant in the large pedigree with early onset PDB

WES analysis in the selected pedigree led to the identification of 10 candidate variants. After excluding common SNPs and variants registered in genetic databases (bdSNP, NCBI, GnomAD), a single high impact variant was identified in the *PFN1* gene, which encodes for profilin1, a highly conserved regulator of actin-polymerization and cell motility (Figure 2). This variant was identified on chromosome 17p13.2 in exon 2 of *PFN1* and consists in a 4-nucleotides deletion (g.2427_2430delTGAC; cDNA.938_941delTGAC), giving rise to a frameshift mutation (D107Rfs*3), where Asp107 and Lys108 both change into Arginine, followed immediately by a stop codon (Figure 2). This is predicted to lead to an early truncation of the C-terminal part of the protein missing the last 31 residues at its C-terminus. Sanger sequencing, after separately cloning alleles to discriminate chromatograms (as the mutation is carried in heterozygosity) confirmed co-segregation of the mutation with the disease phenotype in all affected family members. Moreover one of the two young and apparently unaffected siblings (subject IV.2) carried the same D107Rfs*3 mutation.

The D107Rfs*3 mutation detected in our pedigree was predicted as pathogenic following the international guidelines of the ACMGG/AP [16]. In particular: i) it consisted of a frameshift mutation; ii) it was absent in any of the public databases of polymorphic variants; iii) it segregated in all the affected, while it was not present in healthy, family members. Moreover, two *in silico* tools, Provean [14] and Mutation_Taster2 [15], were interrogated, and both classified the variant as deleterious. Finally, *in silico* prediction of the 3D structure model showed that in the presence of the D107Rfs*3 mutation profilin1 loses the last beta-strand (β7), the last helix (helix 5) and the three phosphorylation sites T109, Y129 and S137 of the corresponding profilin 1 protein (Figure 2D and 2E).

Clinical and cellular phenotype of *PFN1* mutation carriers

All the affected patients from the pedigree had an early onset and polyostotic form of disease (Table 1). Moreover, the skeletal distribution of lesions was less focal than generally described in PDB, involving the skull, one or more vertebral bodies and the lower limbs in all affected cases (Figure 1). In addition to the distribution of lesions and the early onset, other peculiar characteristics of all the affected patients included the presence of severe osteoarthritis at the spine and major joints, and the occurrence of autoinflammatory diseases (mostly autoimmune thyroiditis). Both conditions, albeit common with aging in the general population, occurred at a relatively young age in all the affected subjects (between 25 and 50 years). Three patients (Pt. II.4, II.6 and their affected cousin, Pt. II.9) also reported fractures at or nearby the affected skeletal sites (Figure 1), while the affected male in generation I (Pt. I.2) died at age 63, because of neoplastic degeneration of the pagetic humerus in osteosarcoma. No reported cases of dementia or motor neurone disease (e.g. amiotrophic lateralsclerosis) were present in family history.

After PDB diagnosis, all patients had received intravenous (Pamidronate 30mg/day for 3 days twice/year) and/or intramuscular (Neridronate 25mg/month or 25mg/15 days for 3 years in patient III.4) bisphosphonate treatment, without achieving the normalization of alkaline phosphatase levels, nor the remissions of pain. After they came to our attention, they received a first course of zoledronic acid 5mg with a significant decrease of total and bone alkaline phosphatase levels (Figure 3A) and a reduction of bone pain. However, in contrast to what is generally observed in the majority of PDB patients, the normalization of bone turnover at 1 year was achieved only in 2 of the 5 cases. Moreover, as is evident in Figure 3, multiple zoledronate courses (up to 6 in patient II.2) were required in all cases to control bone pain and achieve biochemical remission over a long term. Likewise, the comparison of scintiscans of patients II.2 and II.4 performed at baseline and, respectively, 5 or 4 years from the beginning of treatment, showed the persistence of tracer uptake after multiple zoledronate courses (Figure 3B and 3C), on the opposite to what observed in classical PDB, where absent or minimal residual disease activity is generally described [17]. Despite these

annual zoledronate infusions, no long term complications of aminobisphosphonate treatment (e.g. jaw osteonecrosis or atypical femoral fractures) were reported.

In vitro osteoclastogenesis from PBMCs of one affected member (Pt.III.4) showed a higher number of osteoclasts with PDB-like features such as a larger size and a higher number of nuclei, compared to a sex- and age-matched healthy control (Figure 4).

PFN1 mutation screening and genotype-phenotype analysis in a cohort of PDB patients

Sequencing of the entire *PFN1* coding region in 41 unrelated patients with early onset, polyostotic PDB and 3 additional cases with pagetic osteosarcoma (for which mutations in all known genes affected in PDB had been excluded) identified the same D107Rfs*3 mutation in one patient. The mutation occurred in a familial PDB case with a referred diagnosis at 40 years and affecting 6 skeletal sites, including the skull.

Genotype-phenotype analysis of the PDB cases with *PFN1* mutation as compared to the other PDB cases from the Italian PDB Registry are summarised in Figure 5A and 5B. As is evident, PDB patients with *PFN1* mutation showed an increased number of affected sites as well as an earlier age at diagnosis than all the other PDB cases, including those with *SQSTM1* or *ZNF687* mutation.

Diagnosis of PDB-like lesions in a young, 17-year old PFN1 mutation carrier

Following the identification of *PFN1* mutation in one (case IV.4) of the two apparently healthy daughters, we first performed a biochemical screening of bone turnover markers that showed an increase of all tested markers in the 17-year old *PFN1* mutation carrier at 2 different time points (Figure 6A). A subsequent radiological screening allowed to detect an initial osteolytic lesion at the tibia together with

hyperostosis of the skull (Figure 6B), highly suggestive for the same PDB-like disorder. Consistent with the clinical features, PBMC-derived osteoclasts from the affected daughter were larger in size

and showed a higher number of nuclei than the unaffected sister (subject IV.3), resembling the PBMC-derived osteoclasts from the other affected cases (Figure 6C).

Functional Studies

In vitro characterization of Profilin1 in osteoclasts: To better understand the effect of the *PFN1* mutation in osteoclasts biology we first performed functional studies on murine osteoclast differentiation. Indeed, as is evident in Figure 2C, there is a remarkable homology between human and mouse profilin 1 (sharing 134/140 identical aminoacids). Profilin 1 was expressed in the murine osteoclast lineage cells, without significant differences throughout all the steps of osteoclast differentiation (Figure 7A).

Silencing of PFN1 in BMM-derived Osteoclasts: Given the nature of the mutation we hypothesized that D107Rfs*3 gives rise to a loss of function mutant that could be mimicked by knocking down profilin1. MCSF-dependent BMMs were collected from a wild type C57BL6 mouse and infected with lentiviral vectors carrying either a control shRNA (Mock) or a specific shRNA directed against mouse *PFN1* mRNA. Osteoclast differentiation from BMMs did not show any difference in the number of formed osteoclasts between cells silenced for Profilin1 or controls. However, an increase in osteoclast size and number of nuclei was observed upon *PFN1* silencing (Figure 7B), indicating a potential effect of the mutation on osteoclastogenesis. Moreover, *PFN1* knockdown osteoclasts showed an increase in resorptive activity when cultured on bone slices (Figure 7B).

Given the role of *PFN1* on actin ring formation and cytoskeleton reorganization we investigated possible structure alterations in *PFN1*-silenced cells marking actin with pahollidin-594 and assessing podosome belts formation and protrusions. Silenced osteoclasts were highly rich in podosomes, filopodia and lamellipodia, compared to control osteoclasts, where we noticed mostly filopodia (Figure 7C). This was further verified by double staining for F-actin and Paxilin, a protein highly expressed in acting ring formation that bridges the podosome cores to the integrins. These

structures, where the actin core is surrounded by a strong Paxilin contour, were mainly noticed in *PFN1* silenced cells, compared to controls (Figure 7D).

DISCUSSION

PDB is an invalidating, progressive and focal disorder of bone metabolism, generally occurring in ageing individuals and showing a clear familial predisposition in up to 40% of cases. During the past two decades mutations in at least 10 genes (*SQSTM1*, *TNFRS11A*, *TNFRSF11B*, *VCP*, *HNRNPA1*, *HNRNPA2B1*, *MATR3*, *TIA1*, *ZNF687*, and *FKBP5*) have been associated to PDB or other rarer disorders showing a clear phenotypic overlap with PDB [1, 13]. While *SQSTM1* actually represents the most common mutated gene in familial cases with "classical", late-onset forms of PDB, the other genes have been more frequently associated with PDB-like disorders that frequently arise in younger individuals and often present peculiar skeletal and extra-skeletal manifestations, in addition to PDB. Moreover, genome-wide studies in large populations of PDB patients identified novel genetic variants (e.g. *OPTN* rs1561570, *RIN3* rs10498635, *TM7SF4* rs2458413) that predispose to the disease [18, 19]. Remarkably, most of the genes associated to date with PDB or PDB-like disorders affect key molecular pathways regulating osteoclast formation and activity, and mutations in these genes have been related with typical phenotypic features observed in pagetic osteoclasts both *in vivo* and *in vitro*. Somewhat unexpectedly, some of these genes (e.g. *SQSTM1*, *VCP* and *OPTN*) have been also implicated in the predisposition for amiotrophic lateral sclerosis, frontotemporal dementia or other neurodegenerative disorders [20-22].

Herein, we report about the identification of a pathogenetic mutation in a new gene, *PFN1*, in affected members from a large pedigree with an early-onset and severe form of PDB. This gene encodes for profilin 1 (also known as *ALS18*, since mutations in this gene have been previously found in familial cases of amiotrophic lateral sclerosis), a highly conserved protein among vertebrates, that is expressed in most tissues, with higher concentrations in lymph-nodes, bone marrow and spleen [23, 24]. It is a member of the profilin family (PFN1-PFN5) of small actin-binding proteins that are

involved in the dynamic turnover and restructuring of the actin cytoskeleton, and thus essential to cell motility, division and morphology [23, 25]. Human Profilin1 has a complex molecular structure: it is composed of 7 beta sheets and 5 helices, that form an actin binding domain, two phosphoinositides (PPIs) binding sites and a poly-L-proline (PLP) binding domain [23, 26]. Regarding actin, its major function consists in promoting its exchange from ADP to ATP, which can both inhibit or promote polymerization by either sequestering actin from the available pool and promote assembly of ATP charged actin. In this respect, profilin 1 negatively regulates actin polymerization at the point end of the filament (rich in ADP-actin), while positively regulates its elongation of the barbed end (where it refills the pool rich in ATP-actin) [27]. Moreover, profilin 1 can also bind proteins with PLP sequences in both the cytosol (e.g. WASP, WAVE, VCP, AF-6, clathrin and huntingtin) and nucleus (p42.POP, SMN, exportin6), all related to regulation of cytoskeleton reorganization, without losing its actin binding capacity [23]. Conversely, the interaction with PPIs recruits Profilin1 to the membrane at the expense of actin binding, so that the two functions cannot co-exist. Since the folded conformation of Profilin1 and its functional domains are not confined to limited regions in the protein (e.g. the actin binding function involves amino acids at both N and C terminus) [28], the detected *PFN1* mutation might have different functional implications. Indeed, at least 8 different *PFN1* mutations have been previously identified in amyotrophic lateral sclerosis, impairing either the actin binding domain (e.g. G118, E117, C71, M114) or the PLP domain (e.g. T109M, Q139L), 6 of which are located in the C-terminal portion and are all lost in the D107Rfs*3 truncated protein [23, 29-33].

Importantly, osteoclasts activity strongly relies on the organization of the actin cytoskeleton that not only allows the cells to move and migrate, but also to resorb bone. In fact, in order to resorb bone, osteoclasts must create the actin ring, a complex and unique structure formed by high-density podosome cores of actin (and regulatory proteins such as cortactin, profilin1, gelsolin) surrounded by actin regulating proteins (e.g. Paxilin, Vinculin) [34, 35]. This structure allows the cells to anchor itself to the bone and seal the region to resorb. Beneath it, at the ruffle border other processes carry

out the resorption: mineral dissolution via the acidification of resorption lacuna and secretion of lysosomal proteases degrading the organic matrix components, whose products are then carried out to the opposing side via transcytosis. All these mechanisms are dependent on cytoskeleton rearrangement [36-39] and thus can be affected by *PFN1* mutation. Indeed, the biology of Profilin1 is complex and its functions, not yet fully characterized, appears context- and cell line- dependent [40]. Notably, several previous experimental evidences have underlined the relevance of profilin 1 for bone biology. While the loss of *PFN1* gene is embryonically lethal (as early as the two-cell stage) [41], conditional knock-out mice models in osteocytes, pre-osteoblasts and osteoclasts are viable and have been recently investigated [42-44]. In particular, osteoclast specific deletion of *PFN1* leads to enhanced cell motility, increased podosome formation, increased size and bone resorptive activity *in vitro*, as well as to different bone abnormalities *in vivo*, including dwarfism, osteolytic lesions and suppressed trabecular bone mass [44].

Results from our functional *in vitro* studies in mutation carriers and BMMS cells are consistent with the above observations and suggest that the frameshift *PFN1* mutation identified in our pedigree confers a loss of function in profilin 1 activity that induces PDB-like features in the osteoclasts, likely due to enhanced cell motility and actin ring formation. Likewise, mixed osteoliyc/osteosclerotic lesions and hyperostotic expansion of the affected bones, together with a marked increase in bone turnover markers, reminiscent of PDB, have been identified in all mutation carriers including a young and apparently unaffected 17-year old relative. Indeed, from an in-depth analysis of radiological and bone scan images of affected cases, the distribution of the lesions appeared more symmetrical and extensive than in classical PDB, involving the skull and all the long bones in most cases. Moreover, the radionuclide bone scans showed a patched-like pattern of tracer uptake at affected bones rather than the uniform uptake typically described in PDB. In some instances tracer uptake was increased in sites without focal bone lesions at radiography, in keeping with a generalized elevation in bone turnover, as also observed in other PDB-like disorders (e.g. familial expansile osteolysis) [13]. These features, together with the very early onset of the lesions

(that possibly might arise in adolescence) and the surprisingly reduced effectiveness of zoledronate treatment, suggest that the disease affecting this pedigree is distinct from classical PDB. In some respects, the radiological and bone scan characteristics resemble Camurati Engelmann disease, but other classic hallmarks of the disease such as muscle weakness, waddling gait, Marfanoid habitus with reduced subcutaneous fat, or systemic manifestations (e.g. anemia, leucopenia) were absent in our pedigree [45]. Moreover, most if not all cases of Camurati Engelmann disease have a mutation in *TGF-β1* gene [45], while a different gene, *PFN1*, was responsible for disease in our pedigree. This is also in keeping with the identification of the same D107Rfs*3 mutation in an unrelated case with early onset, polyostitic PDB from the Italian PDB Registry, suggesting that *PFN1* gene mutation causes a rare and severe PDB-like disorder.

At the time of writing this manuscript, the same D107Rfs*3 mutation in *PFN1* gene has been described in a different PDB pedigree of Italian descent [46]. While the members of our pedigree and the unrelated PDB case carrying the *PFN1* mutation came from the same Italian area (in between Molise and Campania), it is impossible at this stage to exclude the same geographic origin concerning the pedigree of reference 46 , as suggestive of a possible genetic clustering . Consistent with our cases, affected patients of that pedigree had an early onset, polyostotic form of PDB, without a clear information about the affected skeletal sites or the features of the pagetic lesions. Moreover, sarcomatous degeneration was described in 3 cases that, apparently, had only received calcitonin treatment. Given the lack of neoplastic degeneration in our 5 affected cases and in the unrelated patient with the same mutation from our cohort, we can speculate that rather than predisposing to osteosarcoma *per se*, the *PFN1* mutation causes a severe, early onset PDB-like disorder, that if not adequately treated over the long term might increase the risk of sarcomatous degeneration. This is also consistent with the results from epidemiological surveys and systematic reviews of PDB, evidencing a progressive decrease in the prevalence of neoplastic degeneration [3, 47, 48], which in some way coincides with the development of bisphosphonates and particularly of the more potent amino-bisphosphonates. Indeed, all the 3 cases with classical PDB and

osteosarcoma from our large cohort were negative for *PFN1* mutation, but all had severe, long-standing disease.

The recent advances in molecular biology have significantly expanded our understanding of PDB over the last 20 years. It is becoming clearer that different genetic defect are involved in the pathogenetic mechanisms of PDB and PDB-like disorders. Within this context we now present a new PDB-like disorder caused by a rare mutation of *PFN1* gene and presenting a decreased response to amino-bisphosphonate treatment, thus requiring annual zoledronate courses to suppress bone turnover and control bone pain. Genetic screening of individuals with similar clinical features and a particularly earlier onset of PDB is recommended in order to provide an early diagnosis and a more effective targeted treatment.

REFERENCES

1. Gennari L, Rendina D, Falchetti A, Merlotti D. Paget's Disease of Bone. Calcif Tissue Int. 2019;104(5):483-500.

2. Hansen MF, Seton M, Merchant A. Osteosarcoma in Paget's disease of bone. J Bone Miner Res. 2006;21(suppl.2):P58–P63.

3. Rendina D, De Filippo G, Ralston SH, Merlotti D, Gianfrancesco F, Esposito T, Muscariello R, Nuti R, Strazzullo P, Gennari L. Clinical characteristics and evolution of giant cell tumor occurring in Paget's disease of bone. J Bone Miner Res. 2015;30(2):257-263.

4. Gennari L, Rendina D, Picchioni T, Bianciardi S, Materozzi M, Nuti R, Merlotti D. Paget's disease of bone: an update on epidemiology, pathogenesis and pharmacotherapy, Expert Opinion on Orphan Drugs. 2018; 6(8):485-496.

5. Paget J. On a form of chronic inflammation of bones (osteitis deformans). Med Chir Trans 1876; 60:37–63.

6. Corral-Gudino L, Tan AJ, Del Pino-Montes J, Ralston SH. Bisphosphonates for Paget's disease of bone in adults. Cochrane Database Syst Rev. 2017;12:CD004956.

7. Ralston SH, Corral-Gudino L, Cooper C, Francis RM, Fraser WD, Gennari L, Guañabens N, Javaid MK, Layfield R, O'Neill TW, Russell RGG, Stone MD, Simpson K, Wilkinson D, Wills R, Zillikens MC, Tuck SP. Diagnosis and Management of Paget's Disease of Bone in Adults: A Clinical Guideline. J Bone Miner Res. 2019;34(4):579-604.

8. Reddy SV, Menaa C, Singer FR, Demulder A, Roodman GD. Cell biology of Paget's disease. J Bone Miner Res 1999;14(suppl.2):3–8.

9. Galson DL, Roodman GD. Pathobiology of Paget's disease of bone. J Bone Metab. 2014;21(2):85–98.

10. Singer FR. Paget's disease of bone-genetic and environmental factors. Nat Rev Endocrinol. 2015;11(11):662-671.

11. Roodman GD, Windle JJ. Paget disease of bone. J Clin Invest. 2005;115(2):200-208.

12. Divisato G, Formicola D, Esposito T, Merlotti D, Pazzaglia L, Del Fattore A, Siris E, Orcel P, Brown JP, Nuti R, Strazzullo P, Benassi MS, Cancela ML, Michou L, Rendina D, Gennari L, Gianfrancesco F. ZNF687 mutations in severe Paget disease of bone associated with giant cell tumor. Am J Hum Genet 2016;98(2):275–286.

13. Ralston SH, Taylor JP. Rare Inherited forms of Paget's Disease and Related Syndromes. Calcif Tissue Int. 2019;104(5):501-516.

14. Choi Y, Chan AP. PROVEAN web server: a tool to predict the functional effect of amino acid substitutions and indels. Bioinformatics. 2015;31(16):2745-2747.

15. Schwarz JM, Cooper DN, Schuelke M, Seelow D. MutationTaster2: mutation prediction for the deep-sequencing age. Nat Methods. 2014;11(4):361-362.

16. Richards S, Aziz N, Bale S, Bick D, Das S, Gastier-Foster J, Grody WW, Hegde M, Lyon E, Spector E, Voelkerding K, Rehm HL; ACMG Laboratory Quality Assurance Committee. Standards and guidelines for the interpretation of sequence variants: a joint consensus recommendation of the American College of Medical Genetics and Genomics and the Association for Molecular Pathology. Genet Med. 2015; 15: 405-424.

17. Reid IR, Maslowski K. Long-Term Bone Scintigraphy Results After Intravenous Zoledronate in Paget's Disease of Bone. Calcif Tissue Int. 2017;101(1):43-49.

18. Albagha OM, Visconti MR, Alonso N, Langston AL, Cundy T, Dargie R, Dunlop MG, Fraser WD, Hooper MJ, Isaia G, Nicholson GC, del Pino Montes J, Gonzalez-Sarmiento R, di Stefano M, Tenesa A, Walsh JP, Ralston SH. Genome-wide association study identifies variants at CSF1, OPTN and TNFRSF11A as genetic risk factors for Paget's disease of bone. Nat Genet. 2010;42(6):520–524.

19. Albagha OM, Wani SE, Visconti MR, Alonso N, Goodman K, Brandi ML, Cundy T, Chung PY, Dargie R, Devogelaer JP, Falchetti A, Fraser WD, Gennari L, Gianfrancesco F, Hooper MJ, Van Hul W, Isaia G, Nicholson GC, Nuti R, Papapoulos S, Montes J, Ratajczak T, Rea SL, Rendina D, Gonzalez-Sarmiento R, Di Stefano M, Ward LC, Walsh JP, Ralston SH; Genetic Determinants of Paget's Disease (GDPD)

Consortium. Genome-wide association identifies three new susceptibility loci for Paget's disease of bone. Nat Genet. 2011;43(7):685-689.

20. Pensato V, Magri S, Bella ED, Tannorella P, Bersano E, Sorarù G, Gatti M, Ticozzi N, Taroni F, Lauria G, Mariotti C, Gellera C. Sorting Rare ALS Genetic Variants by Targeted Re-Sequencing Panel in Italian Patients: OPTN, VCP, and SQSTM1 Variants Account for 3% of Rare Genetic Forms. J Clin Med. 2020;9(2). pii: E412.

21. Rainero I, Rubino E, Michelerio A, D'Agata F, Gentile S, Pinessi L. Recent advances in the molecular genetics of frontotemporal lobar degeneration. Funct Neurol. 2017;32(1):7-16.

22. Rea SL, Majcher V, Searle MS, Layfield R. SQSTM1 mutations--bridging Paget disease of bone and ALS/FTLD. Exp Cell Res. 2014;325(1):27-37.

23. Alkam D, Feldman EZ, Singh A, Kiaei M. Profilin1 biology and its mutation, actin(g) in disease. Cell Mol Life Sci CMLS. 2017;74(6):967–981.

24. Wu CH, Fallini C, Ticozzi N, Keagle PJ, Sapp PC, Piotrowska K, Lowe P, Koppers M, McKenna-Yasek D, Baron DM, Kost JE, Gonzalez-Perez P, Fox AD, Adams J, Taroni F, Tiloca C, Leclerc AL, Chafe SC, Mangroo D, Moore MJ, Zitzewitz JA, Xu ZS, van den Berg LH, Glass JD, Siciliano G, Cirulli ET, Goldstein DB, Salachas F, Meininger V, Rossoll W, Ratti A, Gellera C, Bosco DA, Bassell GJ, Silani V, Drory VE, Brown RH Jr, Landers JE. Mutations in the profilin 1 gene cause familial amyotrophic lateral sclerosis. Nature. 2012;488(7412):499-503.

25. Carlsson L, Nystrom LE, Sundkvist I, Markey F, Lindberg U. Actin polymerizability is influenced by profilin, a low molecular weight protein in non-muscle cells. J Mol Biol. 1977;15(3):465–483.

26. Metzler WJ, Farmer BT 2nd, Constantine KL, Friedrichs MS, Lavoie T, Mueller L. Refined solution structure of human profilin I. Protein Sci. 1995;4(3):450-459.

27. Mockrin SC, Korn ED. Acanthamoeba profilin interacts with G-actin to increase the rate of exchange of actin-bound adenosine 5'-triphosphate. Biochemistry. 1980;19(23):5359–5362.

28. Schutt CE, Myslik JC, Rozycki MD, Goonesekere NC, Lindberg U. The structure of crystalline profilin-beta-actin. Nature. 1993;365(6449):810–816.

29. Wu CH, Fallini C, Ticozzi N, Keagle PJ, Sapp PC, Piotrowska K, Lowe P, Koppers M, McKenna-Yasek D, Baron DM, Kost JE, Gonzalez-Perez P, Fox AD, Adams J, Taroni F, Tiloca C, Leclerc AL, Chafe SC, Mangroo D, Moore MJ, Zitzewitz JA, Xu ZS, van den Berg LH, Glass JD, Siciliano G, Cirulli ET, Goldstein DB, Salachas F,
Meininger V, Rossoll W, Ratti A, Gellera C, Bosco DA, Bassell GJ, Silani V, Drory VE, Brown RH Jr, Landers JE. Mutations in the profilin 1 gene cause familial amyotrophic lateral sclerosis. Nature. 2012;488(7412):499–503.

30. Ingre C, Landers JE, Rizik N, Volk AE, Akimoto C, Birve A, Hübers A, Keagle PJ, Piotrowska K, Press R, Andersen PM, Ludolph AC, Weishaupt JH. A novel phosphorylation site mutation in profilin 1 revealed in a large screen of US, Nordic, and German amyotrophic lateral sclerosis/frontotemporal dementia cohorts. Neurobiol Aging. 2013;34(6):1708.e1–6.

31. Chen Y, Zheng ZZ, Huang R, Chen K, Song W, Zhao B, Chen X, Yang Y, Yuan L, Shang HF. PFN1 mutations are rare in Han Chinese populations with amyotrophic lateral sclerosis. Neurobiol Aging. 2013;34(7):1922.e21–25.

32. Smith BN, Vance C, Scotter EL, Troakes C, Wong CH, Topp S, Maekawa S, King A, Mitchell JC, Lund K. Al-Chalabi A, Ticozzi N, Silani V, Sapp P, Brown RH Jr, Landers JE, Al-Sarraj S, Shaw CE. Novel mutations support a role for Profilin 1 in the pathogenesis of ALS. Neurobiol Aging. 2015; 36(3):1602.e17–27

33. Freischmidt A, Schöpflin M, Feiler MS, Fleck AK, Ludolph AC, Weishaupt JH. Profilin 1 with the amyotrophic lateral sclerosis associated mutation T109M displays unaltered actin binding and does not affect the actin cytoskeleton. BMC Neurosci. 2015;16:77.

34. Georgess D, Machuca-Gayet I, Blangy A, Jurdic P. Podosome organization drives osteoclast-mediated bone resorption. Cell Adh Migr. 2014;8(3):191-204.

35. Han G, Zuo J, Holliday LS. Specialized Roles for Actin in Osteoclasts: Unanswered Questions and Therapeutic Opportunities. Biomolecules. 2019;9(1). pii: E17.

36. Mulari M, Vaaraniemi J, Vaananen HK. Intracellular membrane trafficking in bone resorbing osteoclasts. Microsc Res Tech. 2003;61:496–503.

37. Saltel F, Destaing O, Bard F, Eichert D, Jurdic P. Apatite-mediated actin dynamics in resorbing osteoclasts. Mol Biol Cell. 2004;15:5231–5241.

38. Luxenburg C, Geblinger D, Klein E, Anderson K, Hanein D, Geiger B, Addadi L. The architecture of the adhesive apparatus of cultured osteoclasts: from podosome formation to sealing zone assembly. PloS One. 2007;2:e179.

39. Arana-Chavez VE, Bradaschia-Correa V. Clastic cells: mineralized tissue resorption in health and disease. Int J Biochem Cell Biol. 2009;41:446–450.

40. Ding Z, Bae Y H, Roy P. Molecular insights on context-specific role of profilin-1 in cell migration. Cell Adhes Migr. 2012;6:442–449.

41. Witke W, Sutherland JD, Sharpe A, Arai M, Kwiatkowski DJ. Profilin I is essential for cell survival and cell division in early mouse development. Proc Natl Acad Sci U S A. 2001;98(7):3832-3836.

42. Miyajima D, Hayata T, Suzuki T, Hemmi H, Nakamoto T, Notomi T, Amagasa T, Böttcher RT, Costell M, Fässler R, Ezura Y, Noda M. Profilin1 regulates sternum development and endochondral bone formation. J Biol Chem. 2012;287:33545–33553.

43. Lin W, Izu Y, Smriti A, Kawasaki M, Pawaputanon C, Böttcher RT, Costell M, Moriyama K, Noda M, Ezura Y. Profilin1 is expressed in osteocytes and regulates cell shape and migration. J Cell Physiol. 2018;233:259–268.

44. Shirakawa J. Kajikawa S, Böttcher RT, Costell M, Izu Y, Hayata T, Noda M, Ezura Y. Profilin 1 Negatively Regulates Osteoclast Migration in Postnatal Skeletal Growth, Remodeling, and Homeostasis in Mice. JBMR Plus. 2019;3:e10130.

45. Van Hul W, Boudin E, Vanhoenacker FM, Mortier G. Camurati-Engelmann Disease. Calcif Tissue Int. 2019 May;104(5):554-560.

46. Scotto di Carlo F, Pazzaglia L, Esposito T, Gianfrancesco F. The Loss of Profilin 1 Causes Early Onset Paget's Disease of Bone. J Bone Miner Res. 2020 Jan 28. doi: 10.1002/jbmr.3964. [Epub ahead of print]

47. Mangham DC, Davie MW, Grimer RJ. Sarcoma arising in Paget's disease of bone: declining incidence and increasing age at presentation. Bone. 2009;44(3):431–436.

48. Mirabello L, Troisi RJ, Savage SA. Osteosarcoma incidence and survival rates from 1973 to 2004: data from the Surveillance, Epidemiology, and End Results Program. Cancer 2009;115(7):1531-1543.

ACKNOWLEDGMENTS

We thank Giovanni Tonon and Ettore Zapparoli from Ospedale San Raffaele for their support and expertise provided in the whole exome sequencing analyses

LEGEND TO THE FIGURES AND TABLES

Figure 1. Pedigree and key radiological and bone scan features of affected members.

Pedigree of the four-generation family with early onset, polyostotic, PDB-like disorder. Circles indicate female family members, and squares indicate male family members; affected patients are indicated with solid figures. Affected and unaffected cases tested with next generation exome sequencing are indicated in bold, as underlined numbers. The radiographs and bone scan images performed in patients II.2, II.4, II.6, III.4 and III.6 point out the extensive skeletal involvement (including the skull and all the long bones in most cases) and the patched-like pattern of tracer uptake at affected bones rather than the uniform uptake typically described in PDB. The age at which the exam was performed is indicated in parentheses.

Figure 2. Identification of the D107Rfs*3 mutation in *PFN1* gene and impacts on Profilin1 structure.

(A) Chromatograms of identified recessive D107Rfs*3 mutation in comparison to the respective sequence in a healthy subject (top); cloned wild-type and altered allele of an affected patient (below). **(B)** C-terminus alignment of wild type and mutated form of *PFN1* cDNA and protein sequence. The 4-nucleotides deletion (g.2427_2430delTGAC; cDNA.938_941delTGAC) is underlined and gives rise to a frameshift mutation predicted to cause an early truncation of the C-terminal part of the protein. **(C)** Alignment of human (P07737) and mouse (P62962) Profilin1, generated through UniProt (https://www.uniprot.org/).

(D) Schematic representation of PFN1 protein domains, including five α-helices and seven β-sheets. Major mutations identified in Amiotrophic Lateral Sclerosis and C-terminal phosphorilation sites are highlighted with arrows; the D107Rfs*3 mutation is predicted to delete the C-terminal portion including α-helic 5, β-sheet 7 along with the three phosphorilation sites. **(D)** Comparison of wild-type

and mutant three-dimensional structures of human PFN1 protein, modelled from Swiss Model (https://swissmodel.expasy.org/).

Figure 3. Long-term effects of zoledronate treatment. Effects of intravenous zoledronate (5mg infusion) on bone alkaline phosphatase (BALP) levels in patients from the PDB-like pedigree are shown in comparison with response rates of a single infusion in the cohort of PDB cases from the Italian PDB Registry (dashed line). Multiple zoledronate courses (indicated as asterisks) were required in all cases with D107Rfs*3 mutation to control bone pain and achieve biochemical remission over a long term. The upper limits of normal BALP levels for pre-menopausal (19 mcg/L) and postmenopausal women (26 mcg/L), respectively, are boxed in grey and given in square brackets (Figure 3A) . Scintiscans at baseline and at 5 or 4 years from the beginning of treatment for patients II.2 and II.4, respectively, showed the persistence of tracer uptake after multiple zoledronate courses (Figures 3B and 3C).

Figure 4. In vitro osteoclastogenesis from PBMC-derived osteoclasts. PBMC-derived osteoclasts from an affected member (Pt. III.4) were increased in number and size as compared from an age- and sex-matched healthy control. Representative TRAP and phalloidin staining images (right) and quantification of number and size of OCs (left).

Figure 5. Genotype-phenotype correlation across different mutations. Subjects with D107Rfs*3 *PFN1* mutation showed an increased number of affected sites and an earlier age at diagnosis than all the other PDB cases from the Italian PDB Registry, including those with *SQSTM1* or *ZNF687* mutation.

Figure 6. Identification of PDB-like disorder in a young (17-yrs old) carrier of *PFN1* mutation.

(A) Serum total and bone alkaline phosphatase levels and CTX levels in young and apparently healthy members IV.3 (12 yrs) and IV.4 (17 yrs) of the pedigree. **(B)** Radiological analysis of subject IV.4 (carrier of *PFN1* D107Rfs*3 mutation), showing skull hyperostosis and loss of bone density in the frontal region with partial loss of the outer table, together with a small diaphyseal lytic lesion of the right tibia.

(C) PBMCs-derived osteoclasts from subject IV.4, carrier of *PFN1* mutation, appear larger and hypernucleated as compared to osteoclast from her unaffected sister (subject IV.3).

Figure 7. Functional in vitro analysis in murine BMMs-derived osteoclasts. (A) PFN1 mRNA expression did not differ throughout murine osteoclastogenesis. **(B)** western blot, TRAP staining (top panels) and blue toluidine on dentin discs (bottom panels) from murine BMMs-derived osteoclasts silenced for *PFN1* (shPFN1) as compared to control shRNA (Mock), scale bar: 100µm. **(C)** Cytoskeleton evaluation of BMMs-derived osteoclasts upon *PFN1* silencing, staining for actin filaments (phalloidin, red) and nuclei (DAPI, blue); white arrows indicate podosome clusters and lamellipodia. **(D)** Cytoskeleton evaluation of BMMs-derived osteoclasts upon *PFN1* silencing, staining for actin filaments (red), paxillin (green) and nuclei (blue), magnification in white square, scale bars: 50µm.

Table 1. Clinical and laboratory data of affected members of the pedigree

Table 1

Patient	Age *(yrs)*	Age at Diagnosis*(yrs)*	Affected sites *(n)*	ALP at diagnosis *(UI/L)*	Height *(cm)*	BMI	PDB symptoms	PDB complications	HAQ-DI score	Age at onset of pain *(yrs)*
II.2	64	49	9	839	150	30.2	Bone pain, Headache	OA *(spine, pelvis)*, hearing loss	0.75	46
II.4	62	31	10	940	145	22.8	Bone pain, Headache	OA *(shoulder, spine, pelvis, knee)*, hearing loss, fracture *(hip)*	1.60	25
II.6	62	42	12	1859	148	29.2	Bone pain, Headache	OA *(spine, pelvis)*, hearing loss, fracture *(spine)*	1.25	37
III.4	36	29	5	685	162	28.9	Bone pain, Headache	OA *(pelvis, knee)*	0.35	27
III.6	33	20	6	726	159	26.5	Bone pain, Headache	OA *(knee, shoulder, spine)*	0.15	33

HAQ-DI: Health Assessment Questionnaire Disability Index

Figure 1

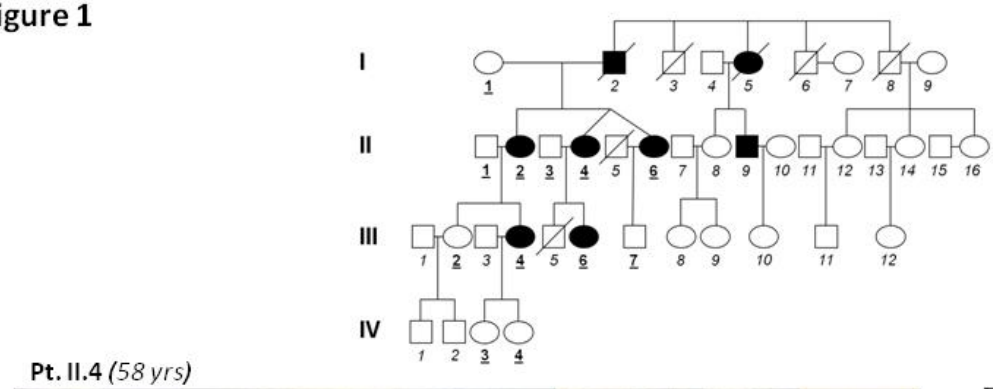

Pt. II.4 *(58 yrs)*

Pt. II.6 *(58 yrs)*

Pt. II.2 *(53 yrs)*

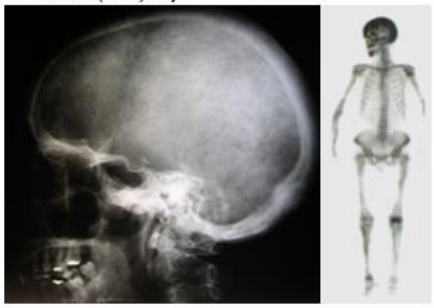

Pt. III.4 *(34 yrs)*

Pt. III.6 *(20 yrs)*

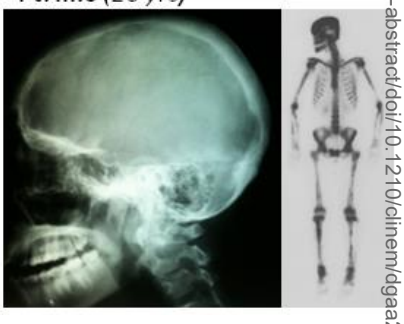

Figure 2

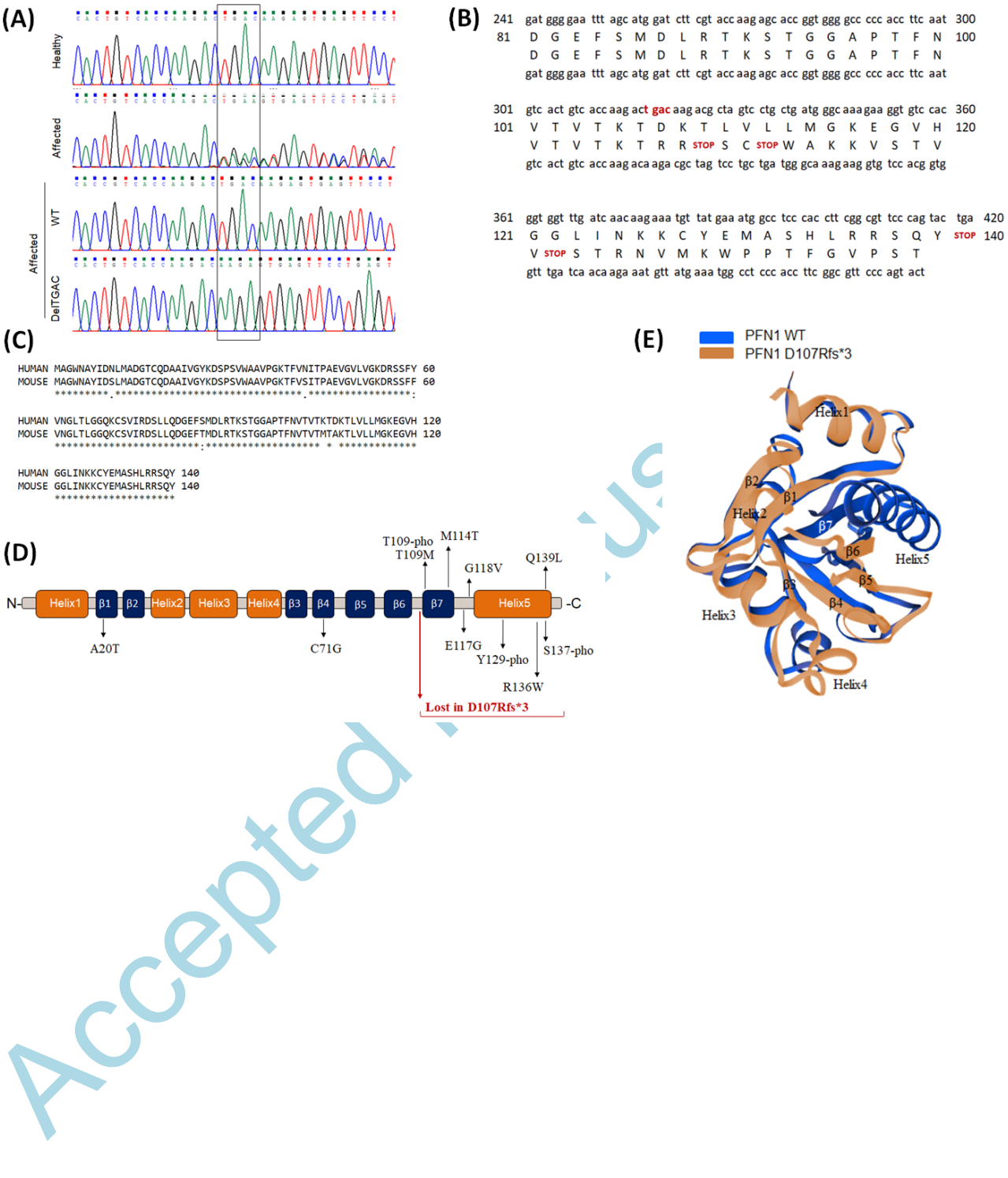

Figure 3

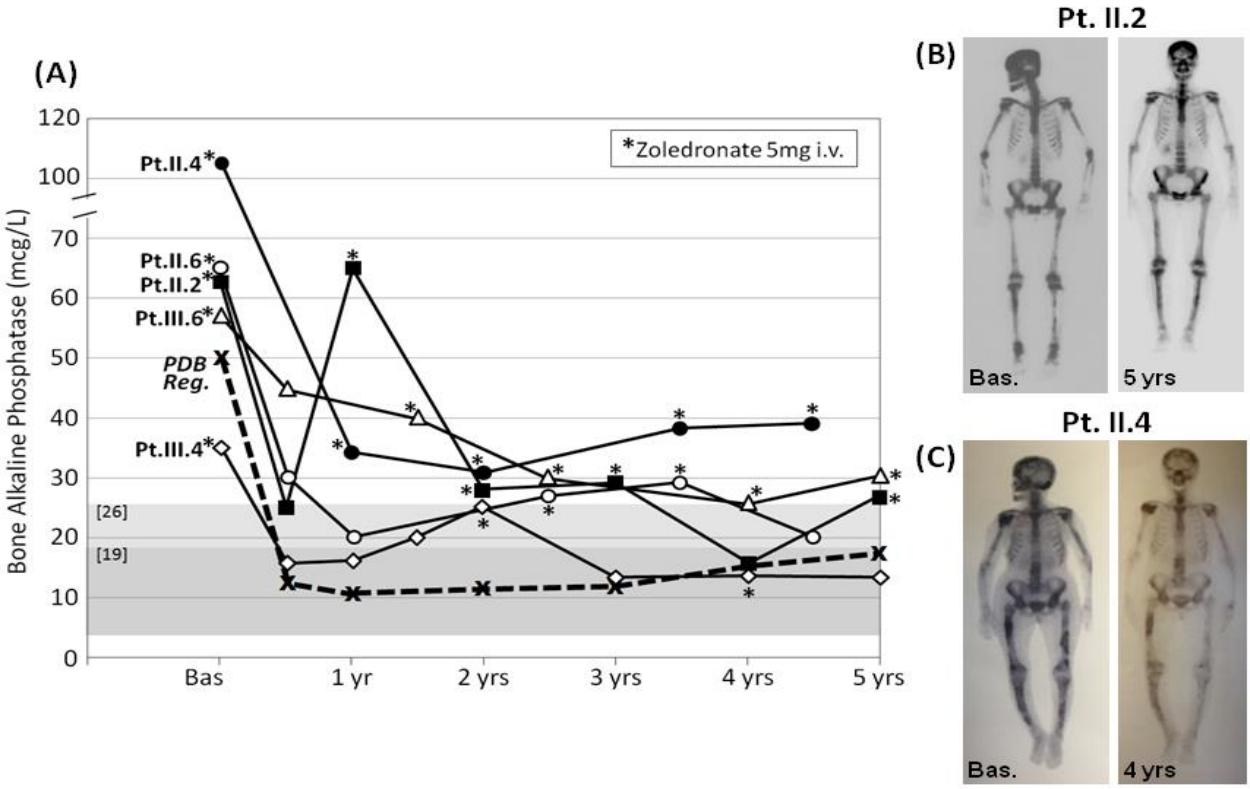

Figure 4

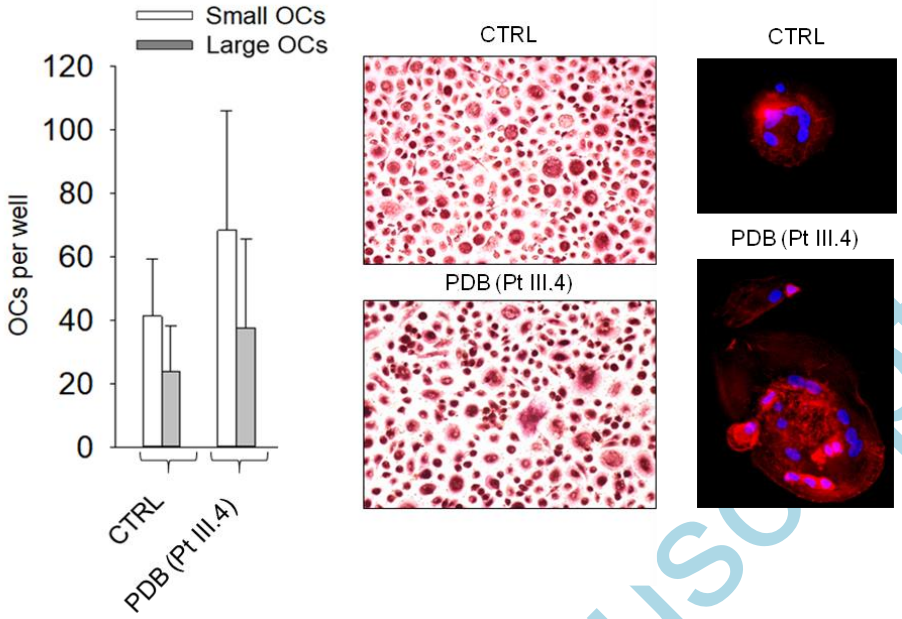

Figure 5

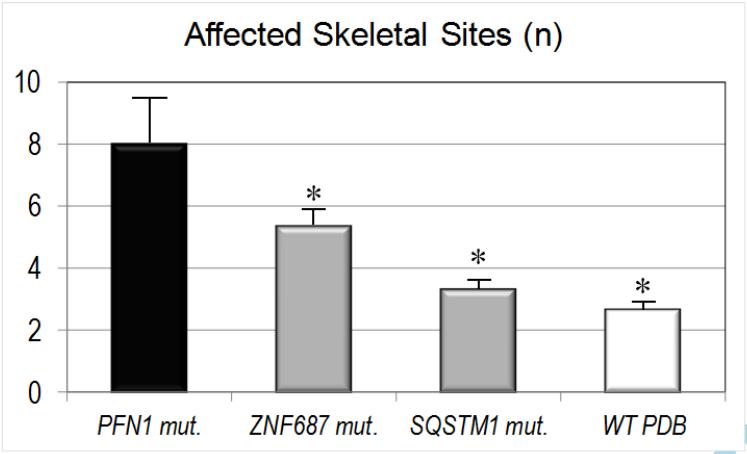

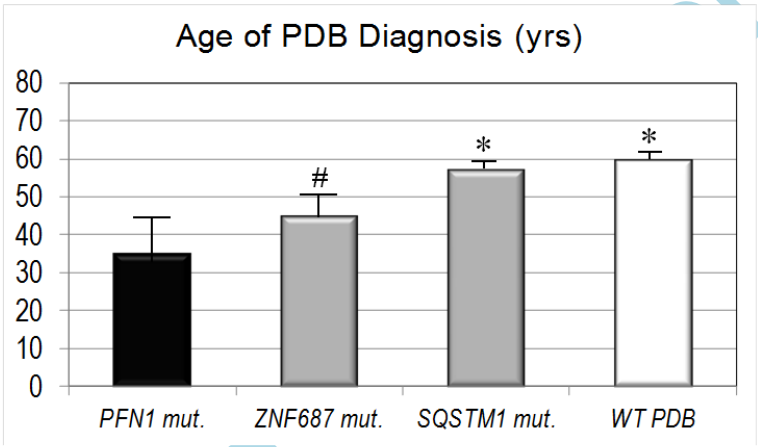

#P<0.05 vs. PFN1 mut. *P<0.01 vs. PFN1 mut.

Figure 6

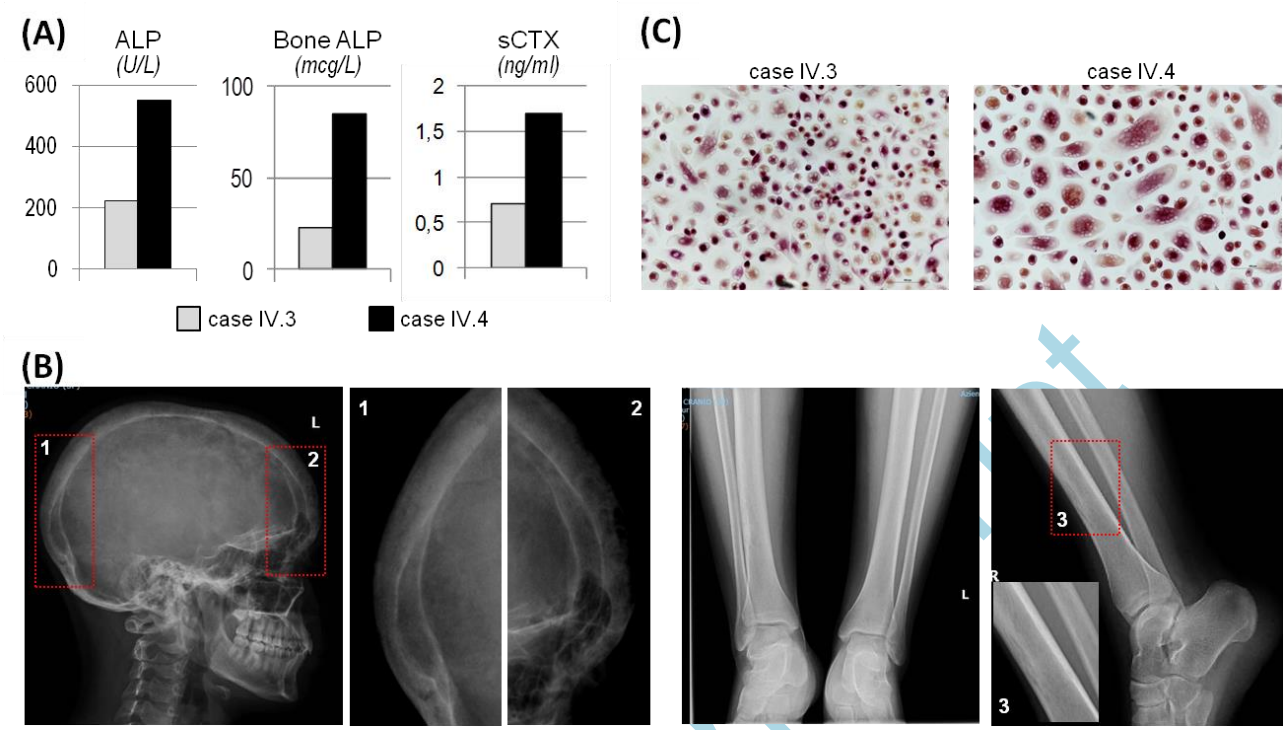

Figure 7